

## Fatigue behaviour and residual service life of existing masonry arch bridges

Michelangelo LATERZA<sup>1</sup>, Michele D'AMATO<sup>2</sup>, Vito Michele CASAMASSIMA<sup>3</sup>

<sup>1,2,3</sup> DICEM, Dept. of European and Mediterranean Cultures: Architecture, Environment and Cultural Heritage.  
University of Basilicata, Matera, Italy

<sup>1</sup> Associate Professor, michelangelo.laterza@unibas.it

<sup>2</sup> Research Fellowship, michele.damato@unibas.it

<sup>3</sup> Phd Student, vito.casamassima@unibas.it

**Abstract:** The conservation and safety assessment of old masonry arch bridges represent nowadays a research field of considerable interest. Most of them are testimonies of the past with a significant historical and cultural value, and represent nowadays a large part of the transport infrastructures serving strategic link for roads and railways networks. In many cases their masonry primary elements are already deteriorated due to weather conditions and to the effects of cyclic traffic loads that are increased in both the frequency and the intensity with respect to the past. Even if the ultimate load is not reached, the cumulated damage along with the localised deterioration can reach levels not acceptable leading the entire structure out of service.

This paper is addressed to the fatigue assessment of old masonry arch bridges with particular attention to the residual service life evaluation of the arch elements. Unlike of metals and metallic structures, little informations are available to date on the fatigue behaviour of masonry elements, also confirmed by the fact that there are no specific guidelines for assessing the fatigue limit and the residual life. The paper at first shows a critical review of the damage models for the fatigue performance assessment of masonry arch bridges. Then, an application to a case study is presented, where also the influence of intradosal C-FRP reinforcement on the residual service life and the ultimate capacity is discussed.

**Keywords:** fatigue behaviour, cyclic load, masonry arch bridges, stress life curves, residual service.

### 1. Introduction

The old masonry arch bridges represent a huge infrastructural heritage asset. It is a duty of the society to conserve these structures for future generations. The bridges are key elements of rail and road networks and their safe maintenance has a strategic importance. Sudden bridge failure or collapse does not only endanger human lives, but also have great economic and environmental consequences, e.g. associated repair costs, road closures, diversions. There are over 220,000 railway bridges in Europe, of which over 35% are more than 100 years old with a further 31% aged between 50 and 100 years. Out of all European railway bridges 60% are masonry, 23% concrete, 22% metallic (Figure 1) Tomor (2013). Similar numbers probably apply for highway bridges. In United States up to 30% of the bridges have been indicated to be structurally deficient or functionally obsolete Tomor (2013). Very often they were built in last centuries and nowadays are exposed to different vehicular traffic conditions compared to the past (the frequency and load intensity are increased).

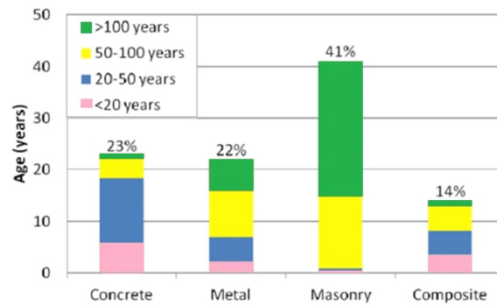


Figure 1 – Railway bridge types and age profile

Usually, these kinds of structures get low attention from the owners, while their conditions increasingly deteriorate. Therefore, the stability control and verification of their bearing capacity become essential in many cases. In order to know the effective traffic capacity and to plan a maintenance strategy of the bridges, it is necessary to evaluate the residual service life related to the actual elements and traffic conditions. At this scope, it should be evaluated not only the ultimate carrying capacity but also the service load that induces in the masonry elements a non-acceptable damage and, therefore, the out-of-service condition of the bridge.

The fatigue assessment of a bridge and the related residual service life may be predicted using behavioral models of masonry capable of simulating the response under cyclic loads. Some fatigue tests have been performed considering the masonry prisms in different load and material conditions Roberts *et al.* (2006), while recently also large-scale fatigue tests on masonry arches have been carried out SB4.7.4. (2007). Research works indicate that the compressive strength under cyclic loads is less than the one measured in the quasi-static way Clark (1994). Based on fatigue experimental tests and regression analyses, some stress-life curves (also indicated usually as S-N curves) have been proposed in literature to evaluate the masonry fatigue response. They predict the number of cycles  $N$  related to the material failure for a given amplitude of the normal compressive stress  $S_a$ . They also provide an endurance limit under which the cyclic strength is infinite. As for design codes, in the British guidelines BD 21/01 (2001) for example a fatigue limit of 50% of the Ultimate Limit State (ULS) is suggested. However, long term fatigue tests on multi-ring masonry arch barrels have indicated that the fatigue limit may be lower than 40% of ULS Melbourne *et al.* 2004, and the permissible limit state PLS may be a more suitable option for identifying residual life for masonry bridges. Conversely, no information regarding this limit is indicated in Italian Code NTC (2008) and EuroCode 6 (2006).

## 2. High-cycle fatigue behaviour of brick masonry

As confirmed by many studies, the compressive strength of masonry under cyclic loads is always less than the one measured in a quasi-static way. This is due to the fact that the cyclic action accelerates the material deterioration due to micro-cracks reducing its carrying capacity. It has been observed, moreover, that the main factors influencing the compressive strength are: the induced stress-range due to vehicular traffic, the frequency of load applied, the degree of saturation of masonry Roberts *et al.* (2006). The earliest tests were undertaken by Clark (1994) on brickwork prisms to study the behaviour of the masonry arches under repeated loading. The fatigue behavior was investigated by testing five course masonry prisms subjected to a central vertical load repeated up to 5 million cycles, with a frequency of 5 Hz. For all test specimens, the minimum cyclic compressive stress was kept at  $0.7 \text{ N/mm}^2$ , corresponding to 5% of the ultimate strength of masonry. Clark observed that dry brick masonry had a fatigue limit of approximately 50% of its quasi-static compressive strength, limit in agreement with the one indicated in the above mentioned British guidelines BD 21/01. (2001).

Ronca *et al.* (2004) performed a series of experimental tests on a number of small-scale masonry specimens. The specimens were cast with a mortar of M4 class, and using brick blocks with the average strength of 48.86 N/mm<sup>2</sup>. The resulting masonry had an average ultimate strength ranged between 10 and 13 MPa. The brickwork prisms were tested under very high vertical loads (65-80% of the ultimate compressive strength) axially applied, and imposing a small variation of the alternating load with three different frequencies: 1, 5, and 10 Hz. The Table 1 reports derived details of all tests conducted where:  $S_{max}$  and  $S_{min}$  are respectively the maximum and the minimum stress in the cycle,  $S_a$  the stress induced to the alternate load, and  $S_u$  the ultimate compressive strength of masonry, the stress ratio  $R$  of  $S_{min}$  to  $S_{max}$ . In Figure 2 are plotted the experimental stress-life curves in terms of  $\log N$  versus  $S_a/S_u$  as reported by the authors, and in the derived form  $\log N$  versus  $S_{max}/S_u$ .

**Table 1** - Masonry parameters investigated by Ronca et al. (2004)

No of samples	f (Hz)	$R=S_{min}/S_{max}$	$S=S_{max}/S_u$	$S_a/S_u$
3	1	0.78	0.9	0.1
3	1	0.83	0.88	0.075
3	1	0.88	0,85	0.05
1	1	0.73	0.75	0.1
2	5	0.73	0.75	0.1
1	10	0.83	0.7	0.05

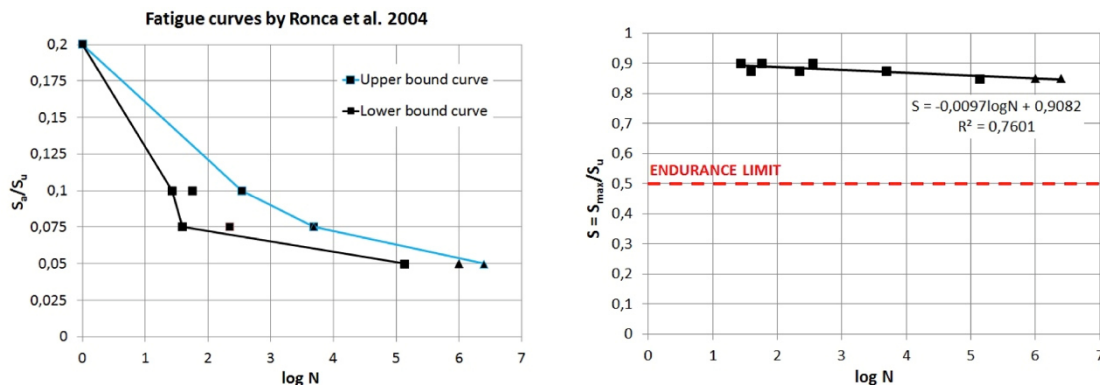


**Figure 2** – Experimental results on masonry specimens subjected to cyclic loads data published by Ronca et al. (2004) (on the left); derived graph in the form of  $\log N$  versus  $S_{max}/S_u$  (on the right).

In Roberts et al. (2006) a series of fatigue tests on the masonry brick specimens were carried out with the aim of establishing the link between the fatigue strength in brick masonry and the fatigue capacity of the masonry arch bridges. They investigated the influence of stress gradient and of saturation degree on the quasi-static and high cycle fatigue strength of brick masonry. The tests were conducted on three types of test specimens for simulating more closely the masonry arch barrel, and considering both dry and saturated conditions. They were applied different vertical load eccentricity ratios  $e/d$  from 0 to 0.256 (where  $e$  is the vertical load eccentricity and  $d$  the specimen depth). During all tests the frequency was typically kept constant to five cycles per second until the specimen failure. As far as the materials details are concerned, the bricks had a mean compressive strength of 18.6 N/mm<sup>2</sup> in dry condition, and of 18.5 N/mm<sup>2</sup> in saturated conditions. Whereas, the mortar was mixed in order to reproduce the representative mortar used for old brick masonry arches. It showed a compressive strength measured at 28 days ranged between 0.45 MPa and 2.78 MPa. The masonry compressive strength determined by assuming a linear stress

distribution along the specimens varied between 6 and 14 N/mm<sup>2</sup>. More details on the specimens and tests set-up may be found in Roberts *et al.* (2006). The authors proposed the following induced stresses function F(S) as shown in equation (1) for describing the fatigue resistance of masonry (Figure 3):

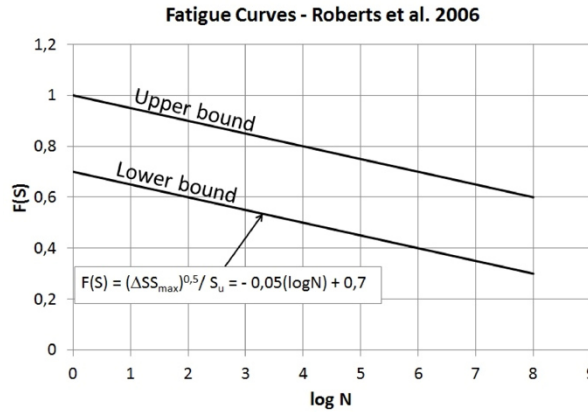


Figure 3 – Upper and lower bond curves proposed by Robert et al. 2006

$$F(S) = \frac{(\Delta SS_{\max})^{0.5}}{S_u} = 0.7 - 0.05 \log N \Rightarrow S = \frac{S_{\max}}{S_u} = \frac{1 - 0.05 \log N}{\sqrt{1 - R}} \quad (1)$$

Starting from the experimental data obtained by Roberts *et al.* (2006), Casas (2009) suggested new fatigue Stress-Life curves derived with a probabilistic approach. By using the Weibull distribution function for describing the progressive fatigue deterioration of brick masonry, has widely used for the analysis of metals and extended for concrete elements, the following fatigue equation was proposed:

$$S = \frac{S_{\max}}{S_u} = A \times N^{-B(1-R)}, \quad S > 0.5 \quad (2)$$

where the coefficients A and B are the fatigue parameters depending on the survival probability, and S=0.5 is the endurance limit. In the case of a survival probability of 95% (i.e. 5% of probability of failure) for masonry in any condition (dry, wet, and submerged) the parameters A and B are equal to 1.106 and 0.1034 respectively. In Figure 4 the stress-life curves derived from the equation 1 and equation 2 are shown for different values of the stress ratio R. An endurance limit can be observed for S = 0.5.

The three stress-life curves considered in this study are compared in Figure 5 in the semi-logarithmic plane LogN - S<sub>max</sub>/S<sub>u</sub> for different values of the ratio R=S<sub>min</sub>/S<sub>max</sub>. In the case of Casas model the stress-life curves are drawn by referring to 95% of survival probability, while the curve proposed by Ronca is plotted for the ratio R=0.8, that is approximately the mean value of R considered in the experimental tests. Also, in all graphs is also indicated the endurance limit S=0.5. By comparing the different stress-life curves it is clear to note that the scatter between the Casas and Roberts curves is significantly reduced for the R ratio comprised among 0.4 and 0.6. Moreover, the Ronca model provides values of the same order of the Roberts and Casas models.

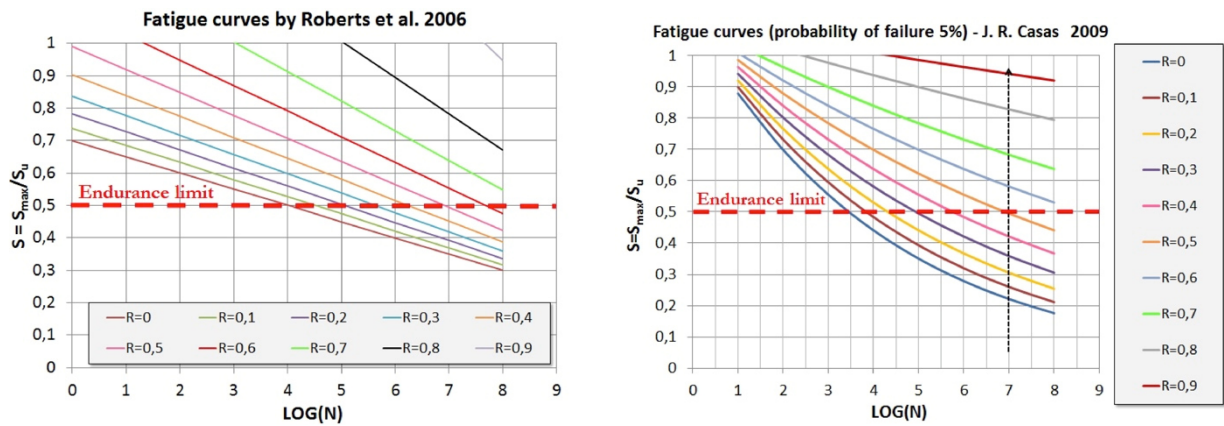


Figure 4 – Derived S-N curves by Robert et al. 2006 and Casas 2009.

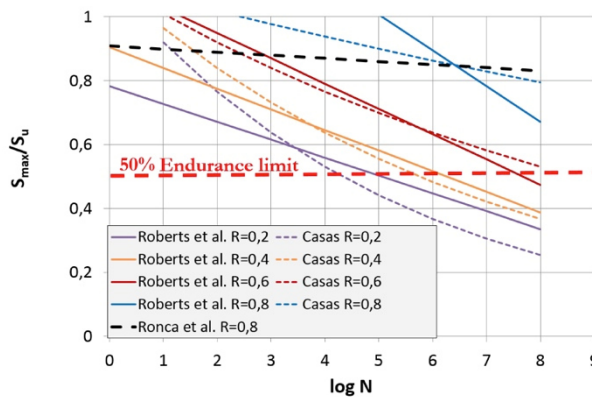


Figure 5 – Comparisons among the fatigue models considered

### 3. Case study: fatigue assessment of Cavone Bridge

The “Cavone bridge” is a multispan masonry arch bridge located in the province of Matera (Figure 6). It is actually in service and was built before the Second World War (approximately during the ‘30s). The bridge takes the name from the crossing river, and consists of seven brick masonry arches covering an overall length of 140 m, with a width of 5.6 m. More in detail, the bridge has three main arches of 22 m span length and four secondary arches of 10 m span length. The three main arches are supported by two piers sunk into the riverbed, having a total height from the foundation plane of about 24 m, of which 14 m above the riverbed. Recently, the bridge has been interested by some in situ tests mainly addressed to identify the materials typology and the elements thickness. In particular, several core samplings in different points have been carried from the bridge deck, reaching in correspondence of the piers 30 m in depth. The in-situ tests have highlighted that the piers consist of an external layer of regular stone blocks containing a core of cohesive backfill. The traffic loads on the roadway spread with depth to the primary arches through an incoherent backfill, confined by the spandrel walls in regular stone blocks. To date, no in-situ test for determining the materials mechanical properties has been performed. Therefore, in the numerical analyses performed in this study the mechanical properties assigned to the bridge elements are those indicated into Italian Code NTC(2008) for existing masonry Circ n.617 (2009).



Figure 6 – Some photos of Cavone Bridge

In this study the fatigue assessment is focused on the main and secondary arches of the bridge. In order to estimate the fatigue performance, the residual service life has been evaluated by using the stress life curves previously discussed. The numerical non-linear analyses have been performed by implementing the arches with fibers elements into OpenSees (2009) and considering the masonry as an uniaxial elastic-perfectly plastic material, having only strength in compression. Moreover, also the influence of C-FRP wraps on the masonry arches has been evaluated by simulating two different interventions: by considering the FRP wraps applied either on the entire extrados or on the entire intrados of arches, having a Young's modulus equal to 230000 MPa, and a total thickness of 0.33 mm (two layers of C-FRP). The C-FRP wraps materials has been assumed as only in tension elastic material up to the rupture, where the maximum tensile stress is associated to the debonding failure, in according to CNR-DT 200/R1 (2013) in this case  $f_{dd}=316$  MPa. In accordance with the Italian Code NTC-08 Instructions (2009), two different values of masonry compressive strength have been considered for the arches. These values are related to two different knowledge levels simulated in this study: for KL1 the assumed strength in compression is equal to 2.40 MPa, while for KL3 the assumed strength is 3.2 MPa. In the analyses the strength  $f$  is also reduced by the confidence factor, equal to 1.35 for KL1, and to 1.0 in the case of KL3. In the Figure 7 are reported the fiber sections adopted for the main and secondary arches, while the uniaxial stress-strain relationship are plotted in Figure 8.

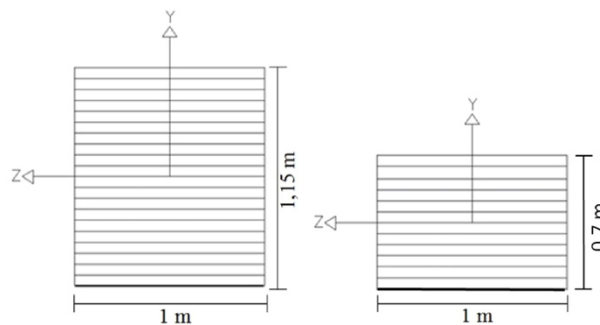


Figure 7 – Fiber section of the main arch (on the left) and of the secondary arch (on the right)

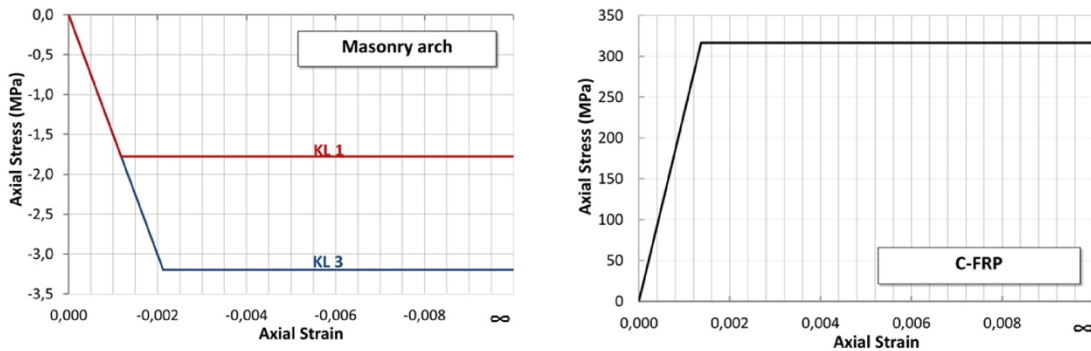


Figure 8 – Materials behavior adopted for the numerical analyses

First step in the fatigue assessment of the two types of arches is the definition of traffic load, that is depending in general on the vehicles geometry, axle loads, vehicle spacing, composition of the traffic and its dynamic effects. In according to the Italian NTC-08 (2008) and Eurocode1 (2003), in this study the Fatigue Load Model 3 is considered (Figure 9), where each axle is equal to 120 kN of vertical load. Moreover, as suggested in the EC1 this fatigue load model is more appropriate for typical heavy traffic on European main roads or motorways. Coherently with the traffic category of the case analyzed, it is assumed a number Nobs of heavy vehicles passing per year on the bridge equal to  $0.5 \times 10^6$  (Figure 9).

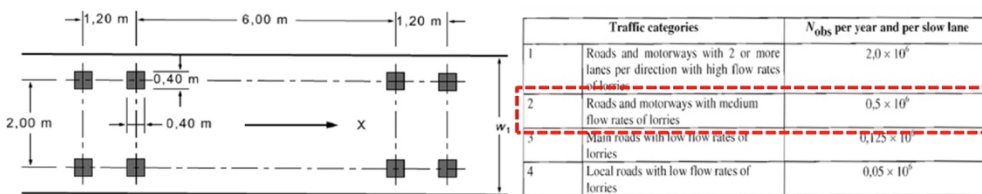


Figure 9 – Fatigue load model 3 (on the left) and traffic categories (on the right)

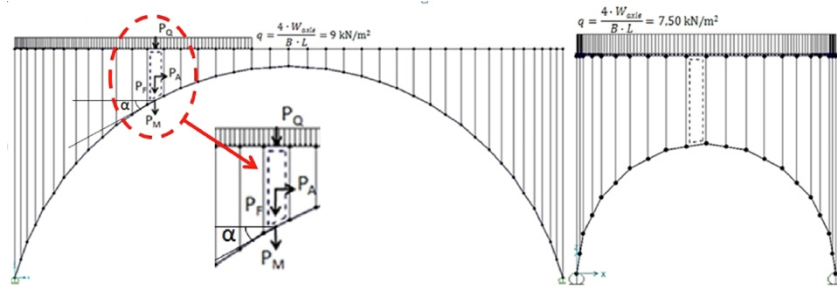


Fig. 10 – Schematization of the loads

The induced stress range  $\Delta\sigma_i$  is evaluated starting from the permanent load condition (self-weight of all elements) by considering the most unfavorable position of the Load Model 3 in terms of compressive stresses. Because there are no particular indications to date in the examined codes for masonry elements, in this study the fatigue assessment procedure proposed in the Italian Code NTC (2008) and also in the EC3 (2003) for steel elements is followed. More in details, in the steel fatigue assessment the stress range  $\Delta\sigma_i$  (due to the stress fluctuation resulting from the transit of the model along the arch) is amplified by  $\gamma_{FF}$ , while the fatigue strength is divided by  $\gamma_{Mf}$  for obtaining from the factored stress-life curve the endurance

value  $N_{Ri}$ . The entire cumulated damage during the design life may be calculated according to Palmgren-Miner's rule (1924) as reported in equation (3):

$$D = \sum_i^n \frac{n_{Ei}}{N_{Ri}} \quad (3)$$

where  $n_{Ei}$  is the number of cycles associated with the stress range  $\gamma_{Ff}\Delta\sigma_i$  for band  $i$  in the factored spectrum expected in certain period (for example the service life);  $N_{Ri}$  is the fatigue endurance (in cycles) obtained from the factored stress-life curve  $\Delta\sigma_c / \gamma_{Mf} - N_R$  for a stress range of  $\gamma_{Ff}\Delta\sigma_i$ . The partial factor for fatigue strength  $\gamma_{Mf}$  takes into account the consequence of the failure and the design assessment used, while  $\gamma_{Ff}$  is a partial factor for equivalent constant amplitude stress range. In this study is assumed that the high consequence of failure arises when the fatigue strength is reached, in conjunction with the fact the masonry arches are not damage tolerant. Therefore,  $\gamma_{Mf}$  is assumed equal to 1.35. The  $\gamma_{Ff}$  partial factor is equal to 1.0 represents the cumulative damage summation, known as Palmgren-Miner rule, and expresses the entire damage cumulated in the examined element when repeated vehicles load transit along the bridge. At the end of service life the fatigue verification is satisfied if the cumulative damage summation  $D$  is less or equal to 1. When  $D$  is greater than 1 then the residual life, related to the remaining cycles up to fatigue failure, may be estimated. In Table 2 and in figure 11 are reported the results of the induced stresses for each supposed knowledge level.

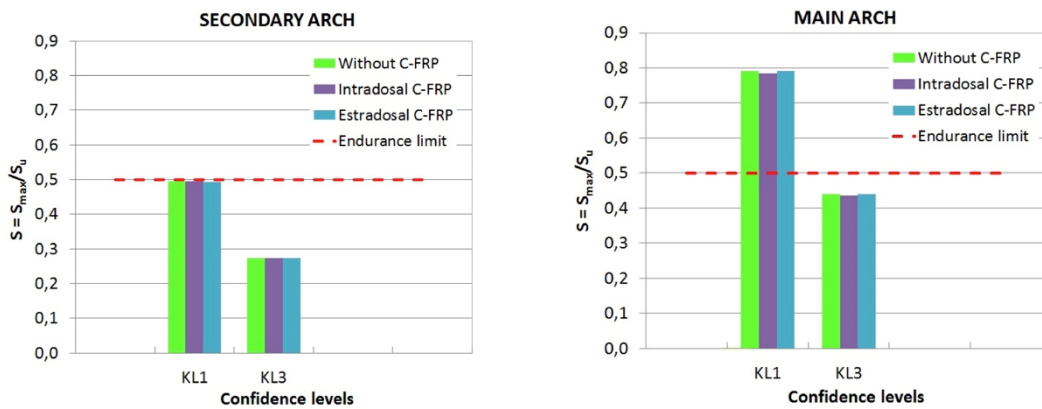


Figure 11 –  $S_{max}/S_u$  ratio obtained by varying the knowledge level of the two arches analyzed.



**Table 2 – Induced compressive stress results**

	Main arch						Secondary arch					
	Without C-FRP		Intradossal C-FRP		Estradosal C-FRP		Without C-FRP		Intradossal C-FRP		Estradosal C-FRP	
Stresses parameters	KL1	KL3	KL1	KL3	KL1	KL3	KL1	KL3	KL1	KL3	KL1	KL3
		2.4/1.35	3.2	2.4/1.35	3.2	2.4/1.35	3.2	2.4/1.35	3.2	2.4/1.35	3.2	2.4/1.35
$S_u$ (MPa)	1.778	3.2	1.778	3.2	1.778	3.2	1.778	3.2	1.778	3.2	1.778	3.2
$S_{max}$ (MPa)	1.405	1.405	1.395	1.395	1.405	1.405	0.878	0.878	0.880	0.880	0.880	0.880
$S_{min}$ (MPa)	1.220	1.220	1.220	1.220	1.220	1.220	0.766	0.766	0.770	0.770	0.760	0.760
$R=S_{min}/S_{max}$	0.868	0.873	0.873	0.873	0.868	0.873	0.872	0.872	0.873	0.872	0.872	0.872
$S=S_{max}/S_u$	0.790	0.440	0.785	0.440	0.790	0.440	0.494	0.275	0.490	0.270	0.490	0.270

In figure 12 and figure 13 are reported the fatigue curves proposed by Roberts et al. (2006), Casas (2009) and Ronca et al. (2004) and the factored ones for the main and secondary arch analyzed in this study by referring to the haunch and key section. It is worth to note that, in the case of secondary arch for knowledge levels KL1 and KL3 and in the case of main arch for KL3 level, the  $S_{max}/S_u$  ratios are always less than the value 0.5, usually indicated as endurance limit. In this case the residual life under cyclic loading can be assumed infinite since the number of load cycles  $N$  related to the fatigue failure are greater than  $10^9$ , and consequently, the residual service life would result greater than 2000 years (the number Nobs of heavy vehicles passing per year is assumed equal to  $0.5 \times 10^6$ ). On the contrary, as shown in table 3 for the main arch, a very low residual life is obtained in the case of KL1 by using Casas and Robert fatigue models. In this case of KL1 for main arch the fatigue model proposed by Ronca cannot be used for both investigated arches because of the ratios  $S_{max}/S_u$  fall beyond the factored stress-life curve. Hence, in this case, no evaluation of the residual life for the arch may be performed with this model. Whereas, the Ronca model provides a residual life that can be substantially considered infinite for main arch in KL3 level and for secondary arch for KL1 and KL3 knowledge levels (Figure 12 and Figure 13).

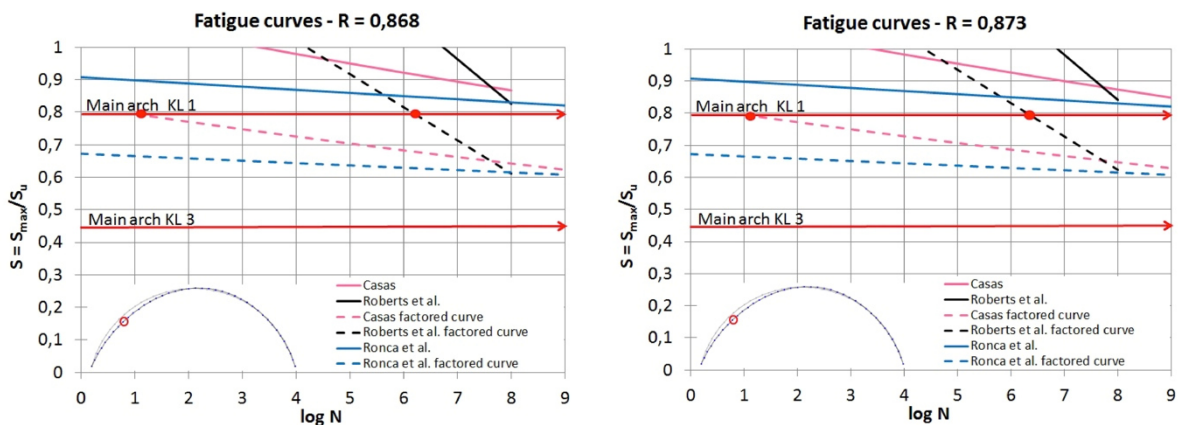


**Figure 12 – Main arch: stress-life curves by Casas (2009) with survival probability of 95%, Roberts et al. (2006) and Ronca et al. (2004) and respectively factored curves.**

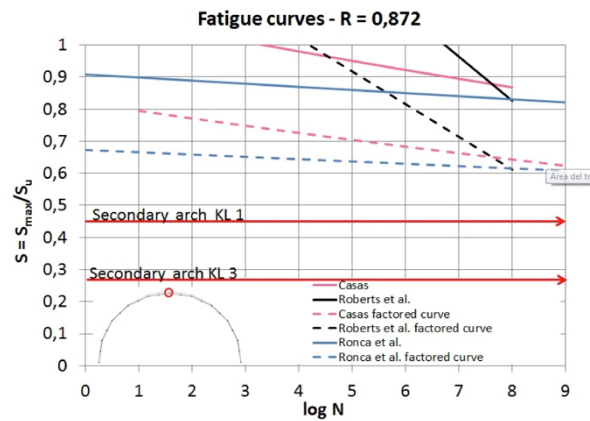


**Figure 13** – Secondary arch: stress-life curves by Casas (2009) with survival probability of 95%, Roberts et al. (2006) and Ronca et al. (2004) and respectively factored curves.

**Table 3** – Residual service life of the main arch in the KL1 knowledge level

Without and estradosal C-FRP - R = 0,868					With intradosal C-FRP - R = 0,873			
S-N curve	Log N	N	(S <sub>max</sub> /S <sub>u</sub> )	Residual life (years)	Log N	N	(S <sub>max</sub> /S <sub>u</sub> )	Residual life (years)
Casas (2009)	1.17	14.63	0.791	0.00003	1.48	30.41	0.785	0.0001
Robert et al. (2006)	6.25	1780025.21	0.790	3.56	6.45	2797211.26	0.785	5.59

It has been also discussed, the influence of C-FRP application to the main arch in terms of carrying capacity and residual service life. The C-FRP has been attached to the intrados and the extrados by varying the debonding failure strength. In the comparisons it is also considered the case in which the debonding failure does not occur and the reinforcement does not applied to the arch.

However, as found in many experiments, debonding can be related to the C- FRP as well, if the masonry C- FRP connection is not strong enough. In addition, some experiments have shown that a debonding failure mode can be accompanied with the four hinges collapse mechanism Foraboschi (2004) introduced by Heyman (1982). Simplified relations and relevant information concerning detachment of the C-FRP, are presented in Foraboschi (2004), Valluzzi (2001). In case that no debonding is permitted in an arch reinforced at the whole length of the intrados, collapse occurs by compressive failure of the masonry. If this is the case, the limit load is considerably increased. Finally, if the reinforcement includes interior C-FRP, the structure is possible to fail by the four hinges mechanism but the positions of the hinges can be different in comparison with the collapse mechanism of the unreinforced arch.

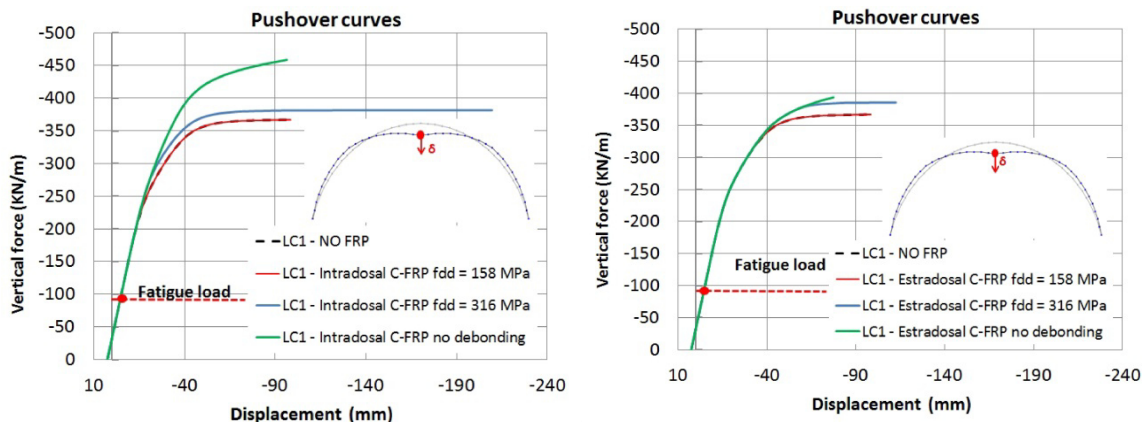


Figure 14 - Main arch: Pushover capacity curves with key displacement control.

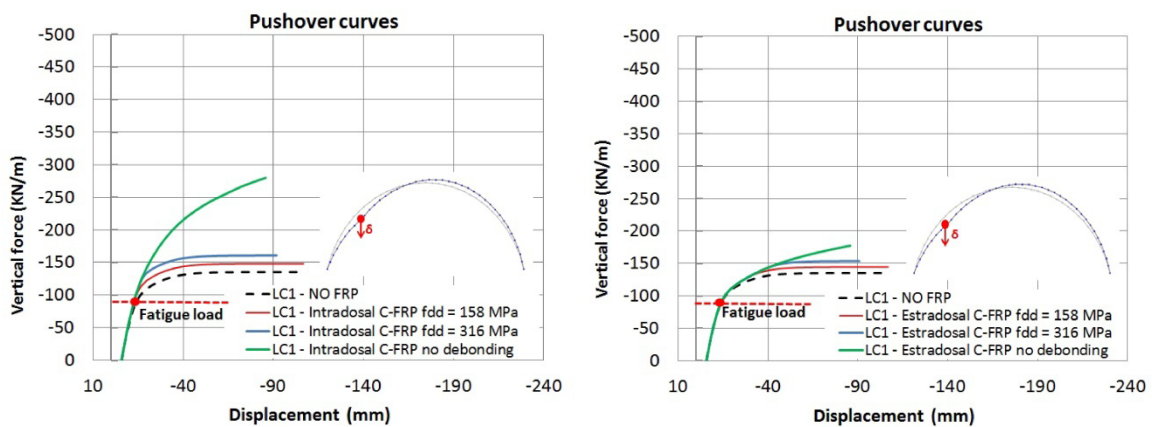


Figure 15 – Main arch: Pushover capacity curves with haunch displacement control.

The results show (table 3) that the residual service life, in the case when C-FRP is placed on the whole length of the extrados does not change compared to the case in which it is not applied. However, when the C-FRP is placed on the whole length of the intrados of the arch the residual service life increases, but not significantly as shown in table 3.

It is noted a small decrease of maximum compression induced stress when the C-FRP is applied to the intrados of the arch. The Figure 14 and Figure 15 show the pushover capacity curves (displacement-vertical reaction) to vary the debonding strength of C-FRP reinforcement. The control point is located to the unfavorable load position, in particular at key and haunch points of the arch. The Figure 14 and Figure 15 show that for the fatigue load model 3 adopted in the analyses, the structure remains elastic and the C-FRP reinforcement has not effect. It should be noted that the ultimate capacity of the arch increases with increasing of the debonding failure strength. When debonding failure does not occurs, the intrados C-FRP reinforcement results more effective in respect to the estradosal C-FRP.

#### 4. Conclusions

A critical review of masonry fatigue models and fatigue assessment procedures of masonry arch bridges are presents. By using fatigue damage models available to date in literature it has been carried out a fatigue assessment of an old existing multi-span Italian masonry arch bridge with backfill above the arches. The fatigue assessment has been focused on the main and secondary arches and the fatigue strength has been expressed in terms of residual service life. The influence of C-FRP reinforcement on the residual service life

and ultimate capacity of the arch elements when the debonding of reinforcement occurs is also discussed. While for steel structures S-N curves and procedures to fatigue assessment are available by considered codes NTC (2008), EC1 (2003) and EC3 (2003), in the case of masonry elements no stress-life curves are proposed.

From the analyses carried out has emerged that all the masonry damage models considered in this study provide very conservative results and the application of C-FRP wraps does not significantly affect neither the fatigue performance nor the ultimate carrying capacity if the debonding failure early occurs. On the contrary, a significant increasing of bearing capacity is obtained when the debonding failure is prevented and especially in the case of intradosal application.

Moreover, in the case analyzed the residual life significantly changes by improving the knowledge level (from a few years to infinite passing from KL1 to KL3 in the case of main arch). This is due, most likely to the fact that the considered stress-life curves Roca *et al.* (2004), Roberts *et al.* (2006,) Casas (2009) have been established from few experimental data, referred to masonry specimens with different compressive strengths. Also, the load frequencies applied during laboratory tests are significantly higher than the ones indicated into NTC (2008) and EC1 (2003) codes for roads and motorways (in the case studied the frequency is equal to 0.015 sec).

Therefore, stress-life curves assume a crucial rule for estimating the residual service life, and it is necessary to define new curves derived for the masonry typical in old existing arch bridges.

## References

- BD 21/01. (2001): Design manual for roads and bridges. The assessment of highway bridges and structures, vol. 3, section 4, part 3. Department of Transport.
- Casas, J.R. (2009). A probabilistic fatigue strength model for brick masonry under compression. *Journal of Construction and Building Material* 23 (8), 2964–72.
- Circolare alle NTC-08 (2009) Circolare, n. 617, 2 febbraio 2009, del Ministero delle Infrastrutture e dei trasporti approvata dal Consiglio Superiore dei Lavori Pubblici “Istruzioni per l’applicazione delle nuove norme tecniche per le costruzioni di cui al D.M. 14 gennaio 2008” (in Italian).
- Clark G.W. (1994). Bridge analysis testing and cost causation project: serviceability of brick masonry. British Rail Research Report LR CES 151;
- CNR-DT 200/R1 (2013): Istruzioni per la Progettazione, l’Esecuzione ed il Controllo di Interventi di Consolidamento Statico mediante l’utilizzo di Compositi Fibrorinforzati. Materiali, strutture di c.a. e di c.a.p., strutture murarie (in Italian).
- D.M. 14 Gennaio (2008). “Norme Tecniche per le Costruzioni”, pubblicato su S.O. n.30 alla G.U. 4 Febbraio 2008, n. 29. (in Italian).
- EN 1991-2 (2003). Eurocode 1. Actions on structures – Part 2: Traffic loads on bridges.
- EN 1993-1-9 (2003). Eurocode 3. Design of steel structures – Part1-9: Fatigue.
- EN 1996-3 (2006). Eurocode 6. Design of masonry structures - Part 3: Simplified calculation methods for unreinforced masonry structures.
- Foraboschi, P. (2004). Strengthening of masonry arches with fiber-reinforced polymer strips. *ASCE J Compos Constr.*, 8(3), 191–202.
- Heyman, J. (1982). The masonry arch. England. Ellis Horwood Series In Engineering Science.
- Melbourne, C., Tomor, A., Wang J. (2004): Cyclic load capacity and endurance limit of multi-ring masonry arches. *Arch Bridges IV Advances in Assessment, Structural Design and Construction*, 375-384.

- OpenSees 2009. <http://openseesnavigator.berkeley.edu/>.
- Palmgren, A.G. (1924): Die Lebensdauer von Kugellagern (Life Length of Roller Bearings. In German). *Zeitschrift des Vereines Deutscher Ingenieure*, 68, 339-341.
- Roberts T.M., Hughes T.G., Dandamudi V.R., Bell B. (2006): Quasi-static and high-cycle fatigue strength of brick masonry. *Journal of Construction and Building Material*, 20, 603-614.
- Ronca P., Franchi A., Crespi A. (2004). Structural failure of historic buildings: masonry fatigue tests for an interpretation model. *Structural Analysis of Historical Constructions*, 273-279.
- SB4.7.4. (2007). Potentiality of probabilistic methods in the assessment of masonry arches. Background document to "Guideline for load and resistance assessment of railway bridges". Prepared by sustainable bridges – a project within EU FP6; <http://www.sustainablebridges.net>.
- Tomor A. (2013). Life-cycle assessment and deterioration models for masonry arch bridges. *The Sustainable City VIII*, 1, 535-546.
- Valluzzi M.R., Valdemarca M., Modena C. (2001). Behavior of brick masonry vaults strengthened by FRP laminates. *ASCE J Compos Constr*, 5(3), 163–9.